Hierarchical Symmetric Normalization Registration using Deformation-Inverse Network

Qingrui Sha[1], Kaicong Sun[1], Mingze Xu[2], Yonghao Li[1], Zhong Xue[3], Xiaohuan Cao[3](✉), and Dinggang Shen[1,3,4](✉)

[1] School of Biomedical Engineering & State Key Laboratory of Advanced Medical Materials and Devices, ShanghaiTech, Shanghai, China
dgshen@shanghaitech.edu.cn
[2] School of Science and Engineering, Chinese University of Hong Kong, Shenzhen, China
[3] Shanghai United Imaging Intelligence Co., Ltd., Shanghai, China
xiaohuan.cao@uii-ai.com
[4] Shanghai Clinical Research and Trial Center, Shanghai, China

Abstract. Most existing deep learning-based medical image registration methods estimate a single-directional displacement field between the moving and fixed image pair, resulting in registration errors when there are substantial differences between the to-be-registered image pairs. To solve this issue, we propose a symmetric normalization network to estimate the deformations in a bi-directional way. Specifically, our method learns two bi-directional half-way displacement fields, which warp the moving and fixed images to their mean space. Besides, a symmetric magnitude constraint is designed in the mean space to ensure precise registration. Additionally, a deformation-inverse network is employed to obtain the inverse of the displacement field, which is applied to the inference pipeline to compose the final end-to-end displacement field between the moving and fixed images. During inference, our method first estimates the two half-way displacement fields and then composes one half-way displacement field with the inverse of another half. Moreover, we adopt a multi-level strategy to hierarchically perform registration, for gradually aligning images to their mean space, thereby improving accuracy and smoothness. Experimental results on two datasets demonstrate that the proposed method improves registration performance compared with state-of-the-art algorithms. Our code is available at https://github.com/QingRui-Sha/HSyN.

Keywords: Symmetric normalization registration · Inverse displacement field · Magnitude constraint · Multi-level architecture.

1 Introduction

Deformable registration is a fundamental task in various medical imaging studies and has been actively investigated for decades [5,20,18]. It involves establishing point-to-point spatial correspondences between the corresponding anatomies, enabling essential applications such as preoperative planning, group-wise analysis,

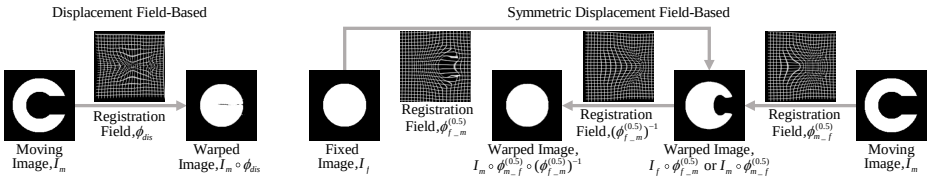

Fig. 1. C-shape controlled experiments. When confronted with image pairs displaying substantial shape variations, our proposed method (right) converts the registration between image pairs into the registration of image pairs to the mean shape, utilizing symmetric displacement fields. The mean shape shares features from both images, facilitating the identification of corresponding points.

and follow-up study [11,19,14]. However, accurately aligning a moving image to a fixed image is often highly challenging when confronted with significant deformations, as shown by a toy example in the left of Fig. 1. The symmetric normalization registration, i.e., registering image pairs to mean shape, yields superior results compared to the case of directly identifying corresponding points between the original image pairs with significant morphological differences.

The symmetric normalization registration (SyN) algorithm has made significant contributions to the field of medical image registration [2]. However, this approach relies on iterative optimization processes to progressively refine the estimation of the displacement field and its inverse version [7,23]. To address the time-consuming nature of SyN, Mok et al. [16] introduce a deep learning-based diffeomorphism network that utilizes a stationary velocity field to derive the displacement field. Although the displacement field and its inverse version can be rapidly obtained through the time-integration of the stationary velocity field, the accuracy of the displacement field based on the velocity field is relatively lower compared to the case of directly estimating the displacement field [6,12,24], and the degradation of performance is further exacerbated in multi-level registration frameworks [17]. Additionally, the displacement field in SyN is defined within the domain of the mean shape, and the domains of mean shapes at different resolutions may not align perfectly. Given the current limitations of deep learning-based registration algorithms, there is an urgent need for the development of a fast and accurate method to register images symmetrically, and meanwhile obtain the inverse displacement field effectively. It is worth noting that our approach aims to symmetrically and progressively register image pairs to an intermediate space rather than directly involving inverse consistency registration between image pairs, as demonstrated by Greer et al. [10].

In this study, we present a novel approach for hierarchical symmetric normalization registration utilizing a deformation-inverse network. Experiments conducted on two datasets demonstrate superiority of our method over several cutting-edge registration networks. The main contributions of our work can be summarized as follows:

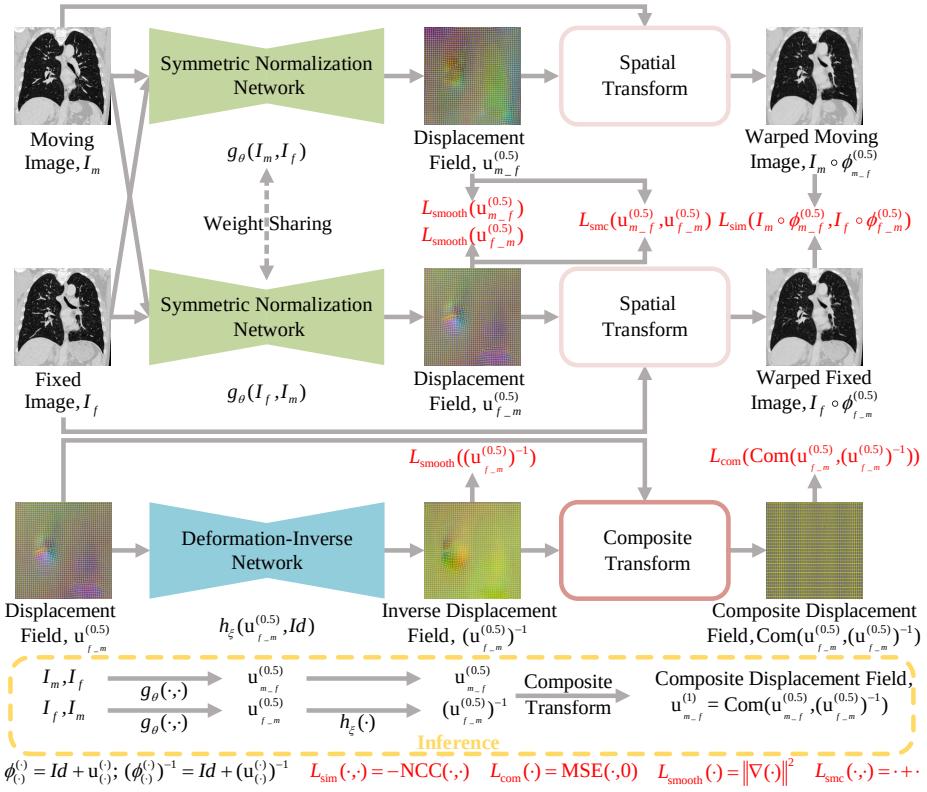

Fig. 2. Schematic illustration of our method. The framework consists of two sub-networks: 1) the symmetric normalization network, which generates symmetric half-way displacement fields, and 2) the deformation-inverse network, which estimates the inverse of the displacement field. During inference, the final displacement field is obtained by composing one half-way displacement field with the inverse of another half (dashed box).

- We propose a symmetric normalization network to align the image pairs symmetrically, which can improve the performance of deformable registration compared with the case of estimating the displacement field in a single direction, especially for image pairs with large local deformations. A symmetric magnitude constraint loss is also designed to encourage the mean shape to be positioned at the middle point.
- We design a deformation-inverse network to enable end-to-end estimation of the inverse displacement field effectively, eliminating the need for reliance on the velocity field. The network is trained based on the fundamental principle that the composition of a displacement field and its inverse version should yield an identity.
- A multi-level symmetric registration framework is applied to align the image pairs hierarchically, which can further enhance both accuracy and robustness.

2 Method

2.1 Network Overview

Fig. 2 presents a schematic representation of our proposed method. The network comprises two sub-networks: 1) the **Symmetric Normalization Network (SN-Net)** and 2) the **Deformable-Inverse Network (DI-Net)**. The SN-Net employs the function $g_\theta(\cdot,\cdot)$ to estimate symmetric half-way displacement fields $\mathbf{u}_{m\_f}^{(0.5)}$ and $\mathbf{u}_{f\_m}^{(0.5)}$ by interchanging the order of moving and fixed images I_m and I_f, thus registering the image pairs into their mean space. During the training stage, the SN-Net warps the image pairs into the mean space, and the similarity loss and regularization loss are defined in this space. On the other hand, the DI-Net utilizes the function $h_\xi(\cdot)$ to estimate the inverse of the input displacement field. The DI-Net is specifically designed to learn the inverse displacement field in an unsupervised manner. In the inference phase, our method first estimates the two symmetrical half-way displacement fields $\mathbf{u}_{m\_f}^{(0.5)}$ and $\mathbf{u}_{f\_m}^{(0.5)}$ using the SN-Net, and then estimate the inverse displacement field $(\mathbf{u}_{f\_m}^{(0.5)})^{-1}$ using the DI-Net. The final displacement field, $\mathbf{u}_{m\_f}^{(1)}$, is obtained by composing $\mathbf{u}_{m\_f}^{(0.5)}$ with $(\mathbf{u}_{f\_m}^{(0.5)})^{-1}$. Subsequently, the moving image I_m is warped using the spatial transform defined by $\mathbf{u}_{m\_f}^{(1)}$.

The two sub-networks are trained independently. The details of these networks and their implementation will be elaborated in the following subsections.

2.2 Symmetric Normalization Network (SN-Net)

The SN-Net is constructed using convolutional neural networks (CNNs) with a similar architecture to VoxelMorph [4]. SN-Net learns parameters θ for the function $g_\theta(\cdot,\cdot)$. In $g_\theta(\cdot,\cdot)$, the image pairs (I_m, I_f) and (I_f, I_m) are provided as a 2-channel input, respectively. The function $g_\theta(\cdot,\cdot)$ generates the symmetric half-way displacement fields $\mathbf{u}_{m\_f}^{(0.5)}$ and $\mathbf{u}_{f\_m}^{(0.5)}$ by interchanging the input order. These displacement fields are subsequently employed to perform spatial transform layer [13], registering the moving and fixed images to their mean shape.

The loss function is designed in the mean space. The basic similarity loss and regularization loss are employed by the normalized cross-correlation $L_{\text{sim}}(\cdot,\cdot)$ [1] and the diffusion regularizer $L_{\text{smooth}}(\cdot)$ [3]. $L_{\text{sim}}(\cdot,\cdot)$ is utilized to penalize dissimilarities between $I_m \circ \phi_{m\_f}^{(0.5)}$ and $I_f \circ \phi_{f\_m}^{(0.5)}$, while $L_{\text{smooth}}(\cdot)$ is employed to penalize spatial gradients of the displacement field.

To ensure the symmetric property, the magnitude constraint is commonly employed to constrain the modulus of the symmetric half-way displacement field, denoted as $L_{\text{mc}} = \frac{1}{|\mathbf{\Omega}|}\sum_{\mathbf{p}\in\mathbf{\Omega}}[||\mathbf{u}_{m\_f}^{(0.5)}(\mathbf{p})||^2 - ||\mathbf{u}_{f\_m}^{(0.5)}(\mathbf{p})||^2]$ [16]. Here, $||\mathbf{u}_{m\_f}^{(0.5)}(\mathbf{p})||^2$ and $||\mathbf{u}_{f\_m}^{(0.5)}(\mathbf{p})||^2$ represent the modulus of the symmetric half-way displacement field. It is crucial to encourage the corresponding anatomical points to be registered at the midpoint rather than loosely aligning them at the perpendicular bisector. Consequently, we modify magnitude constraint loss L_{mc} to a symmetric

magnitude constraint loss L_{smc}. The symmetric magnitude constraint loss can be expressed as follows:

$$L_{\text{smc}}(\mathbf{u}_{m\_f}^{(0.5)}, \mathbf{u}_{f\_m}^{(0.5)}) = \frac{1}{|\mathbf{\Omega}|} \sum_{\mathbf{p}\in\mathbf{\Omega}} [\mathbf{u}_{m\_f}^{(0.5)}(\mathbf{p}) + \mathbf{u}_{f\_m}^{(0.5)}(\mathbf{p})]. \tag{1}$$

Therefore, the final optimization problems for SN-Net can be formulated as follows:

$$\begin{aligned} \theta^* = \underset{\theta}{argmin}\{&L_{\text{sim}}(I_m \circ \phi_{m\_f}^{(0.5)}, I_f \circ \phi_{f\_m}^{(0.5)}) \\ &+ \lambda_1[L_{\text{smooth}}(\mathbf{u}_{m\_f}^{(0.5)}) + L_{\text{smooth}}(\mathbf{u}_{f\_m}^{(0.5)})] + \lambda_2 L_{\text{smc}}(\mathbf{u}_{m\_f}^{(0.5)}, \mathbf{u}_{f\_m}^{(0.5)})\}, \end{aligned} \tag{2}$$

where λ_1 and λ_2 represent the weights of different loss terms.

2.3 Deformable-Inverse Network (DI-Net)

The DI-Net shares a similar architecture to SN-Net and learns parameters ξ for the function $h_\xi(\cdot)$. In $h_\xi(\cdot)$, the displacement field $\mathbf{u}_{f\_m}^{(0.5)}$ serves as a 3-channel input. The function $h_\xi(\cdot)$ generates the inverse displacement field $(\mathbf{u}_{f\_m}^{(0.5)})^{-1}$, which is constrained by a composite similarity loss function L_{com} and a diffusion regularizer loss $L_{\text{smooth}}(\cdot)$ [3].

To construct a composite similarity loss, we first need to obtain the composite displacement field $\text{Com}(\mathbf{u}_{f\_m}^{(0.5)}, (\mathbf{u}_{f\_m}^{(0.5)})^{-1})$ through composite transform. The formalization of this process is as follows:

$$\text{Com}(\mathbf{u}_{f\_m}^{(0.5)}, (\mathbf{u}_{f\_m}^{(0.5)})^{-1}) = \mathbf{u}_{f\_m}^{(0.5)} \circ (\phi_{f\_m}^{(0.5)})^{-1} + (\mathbf{u}_{f\_m}^{(0.5)})^{-1}, \tag{3}$$

where $\mathbf{u}_{f\_m}^{(0.5)} \circ (\phi_{f\_m}^{(0.5)})^{-1}$ represents warping $\mathbf{u}_{f\_m}^{(0.5)}$ with $(\phi_{f\_m}^{(0.5)})^{-1}$ using spatial transform layer.

The solution for the inverse displacement field is based on a fundamental principle: the composition of the displacement field and its inverse version should be equivalent to an identity. Therefore, our composite similarity loss function aims to penalize the mean squared voxelwise difference between the composite displacement field $\text{Com}(\mathbf{u}_{f\_m}^{(0.5)}, (\mathbf{u}_{f\_m}^{(0.5)})^{-1})$ and $\mathbf{0}$. Our loss function can be formulated as follows:

$$L_{\text{com}}(\mathbf{u}_{f\_m}^{(0.5)}, (\mathbf{u}_{f\_m}^{(0.5)})^{-1}) = \text{MSE}(\text{Com}(\mathbf{u}_{f\_m}^{(0.5)}, (\mathbf{u}_{f\_m}^{(0.5)})^{-1}), \mathbf{0}). \tag{4}$$

Therefore, the optimization problems for DI-Net can be formulated as follows:

$$\xi^* = \underset{\xi}{argmin}\{L_{\text{com}}(\mathbf{u}_{f\_m}^{(0.5)}, (\mathbf{u}_{f\_m}^{(0.5)})^{-1}) + \lambda_3 L_{\text{smooth}}((\mathbf{u}_{f\_m}^{(0.5)})^{-1})\}, \tag{5}$$

where λ_3 represents the regularization parameter.

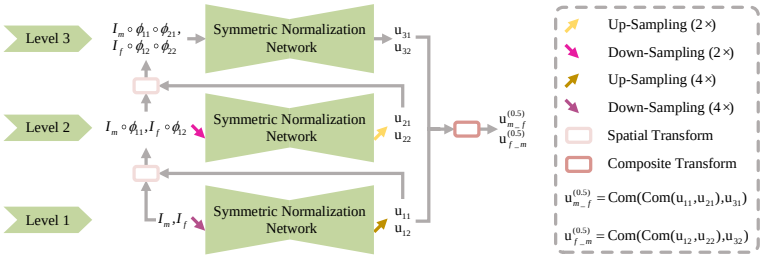

Fig. 3. Implementation of the multi-level architecture for training of symmetric normalization registration.

2.4 Multi-level Architecture

Multi-level registration has proven to be highly effective in both traditional image registration and deep learning-based methods. Following the standard multi-level registration concept, we perform symmetric normalization registration at different resolutions. Our multi-level registration framework, as illustrated in Fig. 3, consists of three levels. The key distinction among the levels lies in the input and resolution of the images. Subsequently, we employ the composite transform on the resulting displacement fields from different levels to derive the final two symmetric half-way displacement fields. Based on this framework, the mean space of fixed and moving images can gradually converge to the middle point, which can facilitate more accurate and smooth registration results.

3 Experiments

Datasets. Experiments are conducted on an in-house chest CT dataset and the publicly available brain MRI dataset OASIS [15]. For chest CT, each patient has two images scanned at different time points, each with annotated lung masks and corresponding pulmonary nodules if available. Some patients have significant respiration, which results in significant deformations in the lung field. The dataset comprises 63 training pairs, 9 validation pairs, and 20 testing pairs. The OASIS dataset consists of 414 T1-weighted volumes and each patient has 35 manually labeled regions of interest. The dataset is divided into training (255 volumes), validation (20 volumes), and test (139 volumes) sets. For each set, five individuals are selected as templates, and the remaining individuals are registered to these templates. Both datasets are resampled to isotropic resolution ($1mm \times 1mm \times 1mm$) and then perform affine registration using FreeSufer [9]. The chest CT images are cropped to the image size of $224 \times 224 \times 192$, while the OASIS images are cropped to the image size of $224 \times 192 \times 160$.

Evaluation Metrics. To quantitatively assess the registration performance, we utilize the Dice Similarity Coefficient (DSC) [3] to evaluate the accuracy, which calculates the degree of overlap between corresponding regions. We also

Table 1. Performance comparison of different registration methods on two datasets.

Methods	CT Dataset			OASIS Dataset	
	DSC(%)↑	TRE(mm) ↓	% of $\lvert J_\phi\rvert \leq 0$ ↓	DSC↑	% of $\lvert J_\phi\rvert \leq 0$ ↓
Affine Only	85.7±6.7	9.5±5.6	-	60.2±15.7	-
ANTs SyN	94.5±2.2	2.4±1.9	< **0.00001**%	77.2±2.8	< **0.0001**%
VoxelMorph	93.1±2.3	3.1±2.1	< 0.001%	78.3±2.6	< 0.02%
TransMorph	94.2±2.4	2.6±2.2	< 0.2%	79.1±2.7	< 0.4%
SYMNet	93.5±2.4	2.8±2.2	< 0.001%	78.5±2.6	< 0.008%
LapIRN	94.8±2.2	1.9±1.5	< 0.1%	80.1±2.5	< 0.7%
ModeT	94.6±2.2	2.1±1.6	< 0.02%	79.3±2.7	< 0.05%
Ours	**95.6 ± 1.9**	**1.5 ± 1.3**	< 0.0002%	**81.2 ± 2.3**	< 0.003%

evaluate the average target registration error (TRE) [22] specifically for pulmonary nodules in the chest CT dataset. The TRE indicates the accuracy of registration within the lung fields. Additionally, the percentage of voxels with a non-positive Jacobian determinant, denoted as $|J_\phi| \leq 0$, is leveraged. This metric can effectively assess the smoothness and topological preserving of the estimated displacement field.

Implementation Details. Our method is implemented using PyTorch, utilizing the NVIDIA Tesla V100 GPU with 32GB memory. The loss weights λ_1, λ_2, and λ_3 are set as 1, 0.1, and 1, respectively. In the case of multi-level training architectures, our three levels of registration are trained progressively. We initiate the training process with the coarse-level networks, training them for a fixed number of iterations before jointly training the three levels together. Additional details can be found at https://github.com/QingRui-Sha/HSyN.

Comparison Methods. We compare our proposed method with the following state-of-the-art registration algorithms: (1) ANTs SyN [2]: A widely recognized traditional approach that uses SyN in the ANTs package. (2) VoxelMorph [8]: A popular deep learning-based registration network. (3) TransMorph [6]: A registration network that combines Swin-Transformer and CNNs. (4) SYMNet [16]: A registration network that employs a velocity field and symmetric strategy for registration. (5) lapIRN [17]: A pyramid architecture-based large deformation registration network. (6) ModeT [21]: A multi-level registration network that utilizes the Transformer for motion decomposition and deformation estimation.

Quantitative and Qualitative Analysis. Table 1 has shown the quantitative results of different methods on the chest CT and OASIS datasets. Our proposed method demonstrates higher registration accuracy on both DSC and TRE metrics, with statistically significant difference. Moreover, the metric $\%\ of\ |J_\phi| \leq 0$ indicates that our method can estimate more smoother displacement field compared with other deep learning-based registration methods. It can well preserve the topology and even register the images with large local deformations. Fig. 4

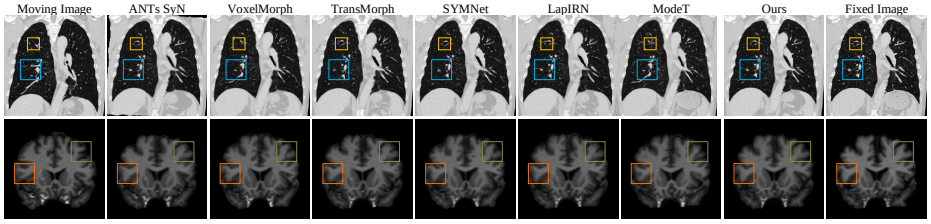

Fig. 4. Visual comparison of registration results by various methods on the chest CT (top row) and OASIS (bottom row) datasets.

Table 2. Ablation experiments of network components. L_{smc}, symmetric magnitude constraint; L_{mc}, magnitude constraint; SN, displacement field-based symmetric normalization registration; MT: multi-level training architecture.

Methods	CT Dataset			OASIS Dataset	
	DSC(%)↑	TRE(mm) ↓	% of $\lvert J_\phi\rvert \leq 0$ ↓	DSC↑	% of $\lvert J_\phi\rvert \leq 0$ ↓
w/o L_{smc} & w/ L_{mc}	94.9±2.2	1.9±1.5	$< 0.0004\%$	80.4± 2.4	$< 0.009\%$
w/o SN	94.6±2.2	2.1±1.6	$< 0.1\%$	80.2±2.5	$< 0.8\%$
w/o MT	94.2±2.4	2.6±2.2	$< 0.0005\%$	79.4±2.5	$< 0.01\%$
w/o SN & MT	93.0±2.3	3.0±2.1	$< 0.001\%$	78.4±2.6	$< 0.02\%$
Ours	$\mathbf{95.6 \pm 1.9}$	$\mathbf{1.5 \pm 1.3}$	$\mathbf{< 0.0002\%}$	$\mathbf{81.2 \pm 2.3}$	$\mathbf{< 0.003\%}$

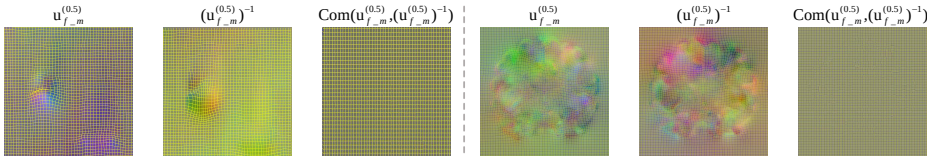

Fig. 5. Illustration of displacement fields, inverse displacement fields, and composite displacement fields for the chest CT (left) and OASIS (right) datasets.

illustrates the visualized registration results obtained by different methods on the two datasets. Our proposed method consistently aligns complex structures well, yielding more precise registered images.

Table 2 presents the numerical results from the ablation study conducted on each component. It can be observed that symmetric magnitude constraint L_{smc} exhibits smoother registration results with fewer voxel folding and higher accuracy compared to the case of using magnitude constraint L_{mc}. Moreover, the inclusion of multi-level training architecture (MT) and displacement field-based symmetric normalization registration (SN) proves to be useful in enhancing accuracy, and their combination leads to further improvements in the final results.

Fig. 5 demonstrates that the effectiveness of the DI-Net. We can see that the composition of the displacement field and its inverse version is close to the identity. Additionally, the mean squared error between $\text{Com}(\cdot,\cdot)$ and $\mathbf{0}$ is below 0.001, indicating sub-pixel level errors in our estimated inverse displacement field.

4 Conclusion

In this study, we have introduced a hierarchical symmetrical registration method using a symmetric normalization network with a deformation-inverse network. Our method effectively addresses challenge of registration for large local deformations. It also facilitates more efficient symmetric registration by introducing a deformation-inverse network to accurately obtain the inverse displacement field. Moreover, a multi-level registration framework is employed to further enhance registration performance. The experimental results have shown the improved performance of our method over representative methods in both accuracy and smoothness.

Acknowledgments. This work was supported in part by National Natural Science Foundation of China (grant numbers 62131015, 62250710165, U23A20295), the STI 2030-Major Projects (grant number 2022ZD0209000), Shanghai Municipal Central Guided Local Science and Technology Development Fund (grant number YDZX2023310 0001001), Science and Technology Commission of Shanghai Municipality (STCSM) (grant number 21010502600), and The Key R&D Program of Guangdong Province, China (grant numbers 2023B0303040001, 2021B0101420006).

Disclosure of Interests. The authors have no competing interests to declare that are relevant to the content of this article.

References

1. Avants, B.B., Epstein, C.L., Grossman, M., Gee, J.C.: Symmetric diffeomorphic image registration with cross-correlation: evaluating automated labeling of elderly and neurodegenerative brain. Medical Image Analysis **12**(1), 26–41 (2008)
2. Avants, B.B., Tustison, N.J., Song, G., Cook, P.A., Klein, A., Gee, J.C.: A reproducible evaluation of ants similarity metric performance in brain image registration. Neuroimage **54**(3), 2033–2044 (2011)
3. Bajcsy, R., Kovačič, S.: Multiresolution elastic matching. Computer Vision, Graphics, and Image Processing **46**(1), 1–21 (1989)
4. Balakrishnan, G., Zhao, A., Sabuncu, M.R., Guttag, J., Dalca, A.V.: Voxelmorph: a learning framework for deformable medical image registration. IEEE Transactions on Medical Imaging **38**(8), 1788–1800 (2019)
5. Cao, X., Yang, J., Zhang, J., Nie, D., Kim, M., Wang, Q., Shen, D.: Deformable image registration based on similarity-steered cnn regression. In: Medical Image Computing and Computer Assisted Intervention- MICCAI 2017: 20th International Conference, Quebec City, QC, Canada, September 11-13, 2017, Proceedings, Part I 20. pp. 300–308. Springer (2017)
6. Chen, J., Frey, E.C., He, Y., Segars, W.P., Li, Y., Du, Y.: Transmorph: Transformer for unsupervised medical image registration. Medical Image Analysis **82**, 102615 (2022)
7. Crum, W.R., Camara, O., Hawkes, D.J.: Methods for inverting dense displacement fields: Evaluation in brain image registration. In: Medical Image Computing and Computer-Assisted Intervention–MICCAI 2007: 10th International Conference, Brisbane, Australia, October 29-November 2, 2007, Proceedings, Part I 10. pp. 900–907. Springer (2007)

8. Dalca, A.V., Balakrishnan, G., Guttag, J., Sabuncu, M.R.: Unsupervised learning for fast probabilistic diffeomorphic registration. In: Medical Image Computing and Computer Assisted Intervention–MICCAI 2018: 21st International Conference, Granada, Spain, September 16-20, 2018, Proceedings, Part I. pp. 729–738. Springer (2018)
9. Fischl, B.: Freesurfer. Neuroimage **62**(2), 774–781 (2012)
10. Greer, H., Tian, L., Vialard, F.X., Kwitt, R., Bouix, S., San Jose Estepar, R., Rushmore, R., Niethammer, M.: Inverse consistency by construction for multistep deep registration. In: International Conference on Medical Image Computing and Computer-Assisted Intervention. pp. 688–698. Springer (2023)
11. Haouchine, N., Dorent, R., Juvekar, P., Torio, E., Wells III, W.M., Kapur, T., Golby, A.J., Frisken, S.: Learning expected appearances for intraoperative registration during neurosurgery. In: International Conference on Medical Image Computing and Computer-Assisted Intervention. pp. 227–237. Springer (2023)
12. Huang, W., Yang, H., Liu, X., Li, C., Zhang, I., Wang, R., Zheng, H., Wang, S.: A coarse-to-fine deformable transformation framework for unsupervised multicontrast mr image registration with dual consistency constraint. IEEE Transactions on Medical Imaging **40**(10), 2589–2599 (2021)
13. Jaderberg, M., Simonyan, K., Zisserman, A., et al.: Spatial transformer networks. Advances in Neural Information Processing Systems **28** (2015)
14. Lorenzi, M., Ayache, N., Pennec, X.: Schild's ladder for the parallel transport of deformations in time series of images. In: Biennial international conference on information processing in medical imaging. pp. 463–474. Springer (2011)
15. Marcus, D.S., Wang, T.H., Parker, J., Csernansky, J.G., Morris, J.C., Buckner, R.L.: Open access series of imaging studies (oasis): cross-sectional mri data in young, middle aged, nondemented, and demented older adults. Journal of cognitive neuroscience **19**(9), 1498–1507 (2007)
16. Mok, T.C., Chung, A.: Fast symmetric diffeomorphic image registration with convolutional neural networks. In: Proceedings of the IEEE/CVF conference on computer vision and pattern recognition. pp. 4644–4653 (2020)
17. Mok, T.C., Chung, A.C.: Large deformation diffeomorphic image registration with laplacian pyramid networks. In: Medical Image Computing and Computer Assisted Intervention–MICCAI 2020: 23rd International Conference, Lima, Peru, October 4–8, 2020, Proceedings, Part III 23. pp. 211–221. Springer (2020)
18. Sha, Q., Sun, K., Jiang, C., Xu, M., Xue, Z., Cao, X., Shen, D.: Detail-preserving image warping by enforcing smooth image sampling. Neural Networks p. 106426 (2024)
19. Shrestha, P., Xie, C., Shishido, H., Yoshii, Y., Kitahara, I.: X-ray to ct rigid registration using scene coordinate regression. In: International Conference on Medical Image Computing and Computer-Assisted Intervention. pp. 781–790. Springer (2023)
20. Siebert, H., Hansen, L., Heinrich, M.P.: Fast 3d registration with accurate optimisation and little learning for learn2reg 2021. In: International Conference on Medical Image Computing and Computer-Assisted Intervention. pp. 174–179. Springer (2021)
21. Wang, H., Ni, D., Wang, Y.: Modet: Learning deformable image registration via motion decomposition transformer. In: International Conference on Medical Image Computing and Computer-Assisted Intervention. pp. 740–749. Springer (2023)
22. West, J., Fitzpatrick, J.M., Wang, M.Y., Dawant, B.M., Maurer Jr, C.R., Kessler, R.M., Maciunas, R.J., Barillot, C., Lemoine, D., Collignon, A., et al.: Comparison

and evaluation of retrospective intermodality brain image registration techniques. Journal of computer assisted tomography **21**(4), 554–568 (1997)
23. Wodzinski, M., Müller, H.: Invnet: A deep learning approach to invert complex deformation fields. In: 2021 IEEE 18th International Symposium on Biomedical Imaging (ISBI). pp. 1302–1305. IEEE (2021)
24. Zhu, Y., Lu, S.: Swin-voxelmorph: A symmetric unsupervised learning model for deformable medical image registration using swin transformer. In: International Conference on Medical Image Computing and Computer-Assisted Intervention. pp. 78–87. Springer (2022)